Title

A THEORETICAL COMPARISON OF FLOW-THROUGH AND FLOW-BY POROUS ELECTRODES AT THE LIMITING CURRENT

Authors

Risch, T. K.
Newman, J.

Publication Date

1984

Lawrence Berkeley Laboratory
UNIVERSITY OF CALIFORNIA

Materials & Molecular Research Division

Submitted to the Journal of the Electrochemical Society

A THEORETICAL COMPARISON OF FLOW-THROUGH AND FLOW-BY POROUS ELECTRODES AT THE LIMITING CURRENT

T.K. Risch and J. Newman

January 1984

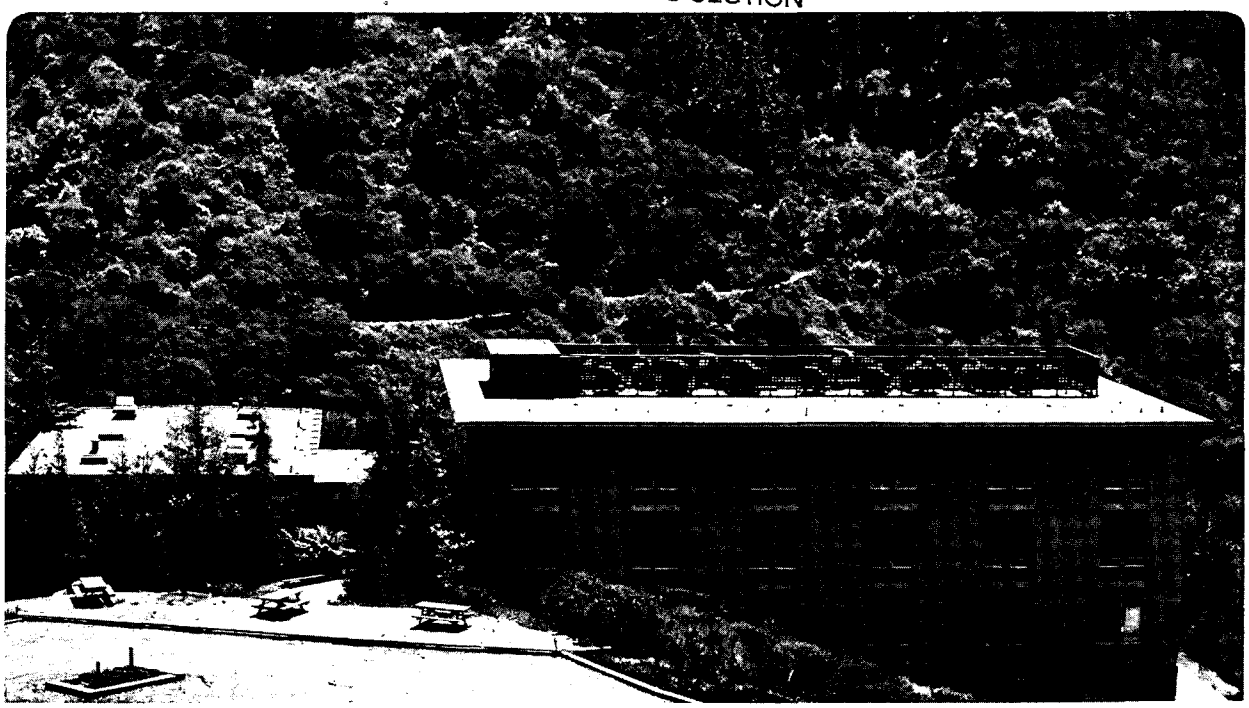

Prepared for the U.S. Department of Energy under Contract DE-AC03-76SF00098

DISCLAIMER

A Theoretical Comparison of Flow–Through and Flow–By Porous Electrodes at the Limiting Current

Timothy K. Risch

Acurex Corporation, Aerotherm Division

Mountain View, California 94039

and

John Newman

Materials and Molecular Research Division

Lawrence Berkeley Laboratory

and

Department of Chemical Engineering

University of California

Berkeley, California 94720

January 26, 1984

Keywords: flow-through porous electrode, potential distribution, optimization

Abstract

A limiting current model for the potential and concentration distribution for a flow–by porous electrode of infinite length to width ratio is developed and compared to previous models of Alkire and Ng and F'edkiw. For flow–by electrodes of practical interest, the maximum solution phase potential drop is shown to be dependent upon one relevant parameter: the product of the electrode width and the reciprocal of the penetration depth, αd. Criteria delineating the optimal electrode configuration are given using this potential difference as a basis for comparison. Results of the comparison show that the criteria are dependent upon reactant conversion but independent of any specific mass transfer correlation.

Introduction

Packed–bed porous electrodes have become increasingly attractive in the past several years for use in a number of industrially important processes. These electrodes have been suggested for such diverse applications as removal of dilute metal ions from waste streams [1], electro–organic synthesis [2], and off–peak energy storage [3].

Two principal configurations for packed–bed electrodes have been developed: the flow–through configuration, where fluid flow and current are parallel; and the flow–by configuration, where the fluid flows perpendicularly to the current. Both configurations are illustrated in Figure 1; where the porous electrodes are represented by rectangles and the separators by dashed lines. For simplicity we choose to represent the counterelectrodes as planar electrodes; however, in general, the counterelectrodes can also be porous electrodes.

Figure 1a illustrates a flow–through electrode with an upstream counterelectrode. An upstream counterelectrode is favored over a downstream counterelectrode in the flow–through configuration, because it gives a lower ohmic potential drop, particularly at high conversions [4]. The y direction denotes the direction of fluid flow in the figure. For the flow–through configuration, the flow is divided as it enters and flows in different directions through the working electrode and counterelectrode. Current generated within the porous electrode flows in the same spatial direction as the fluid flow.

Figure 1b illustrates a flow–by configuration. For the flow–by configuration the fluid flow is again divided, but here the flow to the working

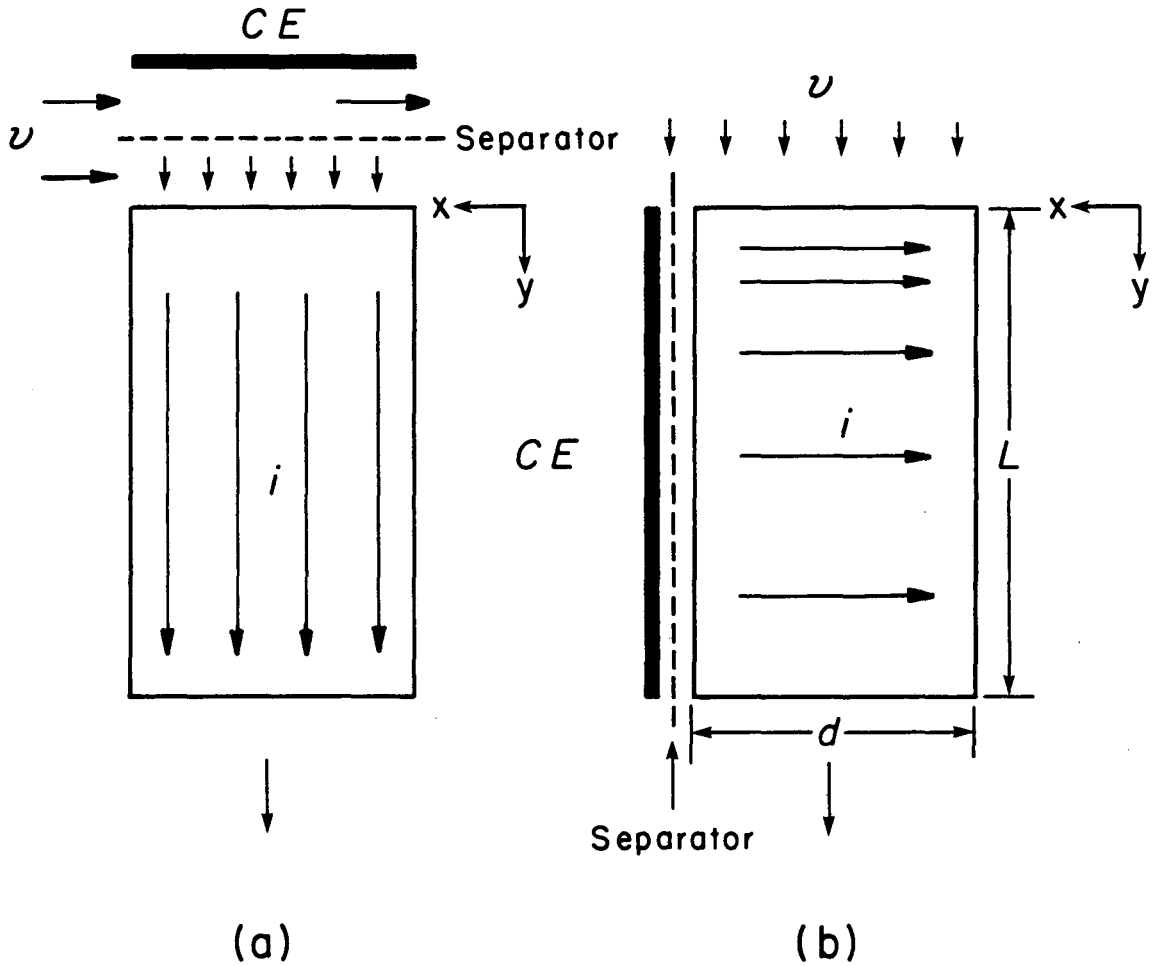

Figure 1

electrode and counterelectrode remains in the same direction. In this configuration, current generated within the porous electrode travels generally in the x direction, which is perpendicular to the direction of the fluid flow.

Bennion and Newman [1] developed a one–dimensional model for the flow–through electrode assuming its performance to be limited only by the transport of reactants from the bulk stream to the surface of the electrode. More realistic one–dimensional models for the flow–through electrode not restricted to this "limiting current" assumption have subsequently been developed [5]. These models incorporate equilibrium constraints, finite rate kinetics, and parasitic side reactions in addition to the transport of reactants.

Because the fluid and current travel in the same direction in the flow–through configuration, the analysis remains one–dimensional even in the general case. In the flow–by configuration, however, the general analysis is necessarily two–dimensional. The absence of a common space variable for the fluid and current flow requires that the analysis be formulated in terms of partial differential equations unless simplifications are made.

Alkire and Ng [6,7] simplified the analysis of the flow–by electrode by assuming current flow to travel directly perpendicular to the fluid flow. This assumption reduces the equation for the potential distribution from a partial differential equation to an ordinary differential equation. Recently, Fedkiw [8] has analyzed the special case of a flow–by electrode at the limiting current by including the two–dimensional nature of the current distribution and the effects of the finite electrode length. However, he

included in his analysis a single specific dependence of the mass–transfer coefficient on velocity.

Alkire and Ng [6,7], Trainham and Newman [2], and Fedkiw [8] have all considered the selection of the optimum electrode configuration for a given application. Trainham and Newman developed a method, applicable below the limiting current, to select the optimum configuration. Alkire and Ng, followed by Fedkiw, considered the choice of the optimum configuration at the limiting current. Alkire and Ng maximized the volumetric current density to compare the two configurations. Fedkiw compared the maximum solution–phase potential drop for the flow–through configuration to the maximum solution phase potential for the flow–by electrode. Equal electrode volumes and identical flow velocities were chosen as fixed quantities for these two comparisons. At the limiting current, the maximization of the volumetric current density or the minimization of the maximum ohmic potential drop lead to the same result.

The results of Alkire and Ng and Fedkiw can be reconciled by an order of magnitude analysis. This can be useful in determining the approximate conditions under which the flow–by configuration is superior to the flow–through configuration at the limiting current. Consider a flow–through and a flow–by electrode of equal dimensions and feed flow rates and with identical packings and feed compositions. Each reactor has a length L, width d, and height W. At the limiting current, the reactant flows through the electrode and reacts at a rate determined solely by the type of packing and the magnitude of the fluid flow. The distribution of the reaction and the total current will therefore be identical in the two reactors. For high conversions of reactant to product, most of the reactant will be

depleted in a region very near the front of the electrode. The characteristic length of this region is the penetration depth, denoted by $1/\alpha$. Most of the current in the flow–through electrode with an upstream counterelectrode, must travel an approximate distance $1/\alpha$, through an area of Wd. The majority of the current in the flow–by electrode, however, need only travel a distance comparable to the width of the electrode d, through an area of W/α. The superior electrode configuration is the configuration that yields a lower ohmic potential drop. The ohmic potential drop is the product of the total current times the length of travel divided by the cross sectional area to current flow. A comparison of the ohmic drop shows that the flow–by electrode configuration is preferred for high conversions if the approximate condition

$$\alpha d < 1 \tag{1}$$

is satisfied. This result is identical to the result obtained by Alkire and Ng when they maximized the volumetric current density to compare configurations.

At low conversions however, the penetration length eventually becomes comparable to the electrode length. In this limit, the current in the flow–through electrode now flows a distance L, rather than $1/\alpha$. Likewise in the flow–by electrode, the current flows through an area of WL. Equating the ohmic potential drop in the low–conversion limit results in the criterion that the flow–by configuration is favored for

$$\frac{L}{d} > 1 . \tag{2}$$

Equation 1 shows that, at high conversions, the parameter αd is of primary importance in distinguishing the optimum electrode configuration and in determining the maximum potential drop in the flow–by configuration. At

low conversions, Equation 2 shows L/d can be expected to be the parameter of primary importance in determining the optimum configuration.

In this paper, we propose a limiting–form solution to the two–dimensional potential distribution for large αd. This solution shows that the maximum solution phase potential drop for the flow–by electrode is primarily dependent upon the parameter αd with only a secondary dependence upon L/d. We then reexamine potential distribution derived by Fedkiw to determine the conditions under which the two–dimensional nature of the current distribution and the effects of the finite electrode should be included. This new solution, along with the expressions derived by Fedkiw and Alkire and Ng, is presented in a form that is not restricted to the single mass–transfer correlation presented by Fedkiw.

Finally, the flow–by and flow–through configurations are compared using the maximum solution phase potential drop as a basis for comparison. Criteria are given delineating the optimum electrode configuration which depend upon reactant conversion. Results of this comparison show that the two configurations can be compared independent of any specific mass transfer relationship.

Potential Distribution

The starting point for the analysis will be the theoretical framework for porous electrodes developed by Bennion and Newman [1] and extended by Newman and Tiedemann [9]. The porous electrode is treated as a superposition of two continua, representing the fluid phase and the solid phase. A single reaction of the form

$$\sum_i s_i M_i^{z_i} \rightarrow ne^- \tag{3}$$

will be assumed to occur within the electrode. Under these assumptions, the electrode reaction appears as a homogeneous source or sink term within the conservation of species equation. A solution with excess supporting electrolyte and a uniform solution conductivity will be assumed as well as a dilute solution of reacting species. Diffusion and dispersion will be neglected. Also, the velocity within the electrode is assumed to be plug–flow, one–dimensional in the y direction only. Under these conditions, at steady state, conservation of the reactant species for both the flow–through and flow–by electrode can be expressed as

$$v \frac{dc}{dy} = -ak_m c \ , \tag{4}$$

with the boundary condition

$$at \ y = 0, c = c_F \ . \tag{5}$$

Solution to Equation (4) subject the boundary condition of Equation (5) yields

$$c = c_F e^{-ay} \ , \tag{6}$$

where

$$\alpha = \frac{ak_m}{v} . \tag{7}$$

The reciprocal of the parameter α can be thought of as a penetration length. The penetration length defines the distance where the reactant is depleted to 1/e of its inlet composition, or, as an order of magnitude, the length of the region where most of the reaction occurs within the electrode.

At the end of the bed ($y=L$), the concentration of the flowing stream will have reacted to the largest extent. Here the concentration of the reactant will be denoted as c_L. Equation (6) then gives at the end of the bed

$$c_L = c_F e^{-\alpha L} . \tag{8}$$

This may be rearranged for αL in terms of the inlet and outlet concentrations as

$$\alpha L = \ln \frac{c_F}{c_L} . \tag{9}$$

Equation (9) shows that the parameter αL effectively specifies the conversion of reactant within the electrode.

Now that the concentration distribution has been established, the solution to the potential distribution may proceed. For a uniform conductivity and negligible diffusion potential, Ohm's law governs the potential distribution within the fluid phase

$$i_2 = - \kappa \nabla \Phi_2 . \tag{10}$$

Faraday's law relates the transfer current to the local rate of mass transfer within the electrode

$$j = \frac{nFak_m c}{s_R} . \tag{11}$$

One must also employ the relationship

$$\nabla \cdot i_2 = j \tag{12}$$

which defines the transfer current as the divergence of the total current.

Substituting the concentration distribution obtained in Equation (6) into Equation (11) and using Equations (10) and (12), we obtain

$$\nabla^2 \Phi_2 = - \frac{nFak_m c_F}{s_R \kappa} e^{-ay} \quad (13)$$

In contrast to the solution for the concentration distribution, the solution to the potential distribution depends upon the electrode configuration.

Bennion and Newman [1] solved Equation (13) for a one–dimensional flow–through electrode. Alkire and Ng [6] solved Equation (13) for the flow–by electrode assuming potential variation only in the direction perpendicular to fluid flow. This assumption reduces Equation (13) from a partial differential equation to an ordinary differential equation. Fedkiw [8] solved Equation (13) for two–dimensional current flow in a flow–by electrode of finite length.

Here, we propose to examine the limiting case of a flow–by electrode with an infinite aspect ratio. Thus our case will reflect the condition

$$R = \frac{L}{d} \rightarrow \infty \, . \quad (14)$$

The potential distribution is obtained by solving Equation (13) subject to the boundary conditions

$$at \;\; y = 0 \, , \; \frac{\partial \Phi_2}{\partial y} = 0 \, , \quad (15)$$

$$as \;\; y \rightarrow \infty \, , \; \frac{\partial \Phi_2}{\partial y} \rightarrow 0 \, , \quad (16)$$

$$at \;\; x = 0 \, , \; \frac{\partial \Phi_2}{\partial x} = 0 \, , \quad (17)$$

and

$$at \;\; x = d \, , \; \Phi_2 = V \, . \quad (18)$$

Solution to Equation (13) by separation of variables subject to the boundary conditions in Equations (15) through (18) yields

$$\frac{\Phi_2 - V}{\frac{nFc_F v^2}{s_R \kappa a k_m}} = \left(\frac{\cos \alpha x}{\cos \alpha d} - 1\right) e^{-ay}$$

$$+ 2\alpha d \sum_{n=0}^{\infty} (-1)^n \left(\frac{1}{\lambda_n^2} - \frac{1}{\lambda_n^2 - (\alpha d)^2}\right) e^{-\lambda_n y/d} \cos \lambda_n x/d \,, \quad (19)$$

where

$$\lambda_n = \frac{(2n+1)\pi}{2} \,. \quad (20)$$

To the designer, the maximum variation in solution phase potential may be a quantity of greater interest rather than the potential distribution within the electrode. To relate the relevant design variables to the maximum variation in solution potential, the results of the potential distribution will be used. For the flow–by electrode configuration, the semi–infinite potential distribution indicates that the maximum solution phase potential drop occurs at the front of the electrode, $y=0$, between the two electrode boundaries, $x=0$ and $x=d$. This is the position where the greatest current is flowing. The maximum solution phase potential difference in dimensionless form is given as

$$\frac{\Phi_2(x=0,y=0) - V}{\frac{nFc_F v^2}{s_R \kappa a k_m}} = \frac{\Delta\Phi_2}{\frac{nFc_F v^2}{s_R \kappa a k_m}} = \frac{\Delta\Phi_2}{\frac{\varepsilon nFc_F D_o}{s_R \kappa}} \frac{Sh}{Pe^2}$$

$$= \frac{1}{\cos \alpha d} - 1 + 2\alpha d \sum_{n=0}^{\infty} (-1)^n \left(\frac{1}{\lambda_n^2} - \frac{1}{\lambda_n^2 - (\alpha d)^2}\right) . \quad (21)$$

This result can be compared to the results obtained by other investigators. The Alkire–Ng approximation gives for the maximum solution phase potential difference

$$\frac{\Phi_2(x=0,y=0) - V}{\frac{nFc_F v^2}{s_R \kappa a k_m}} = \frac{\Delta\Phi_2}{\frac{\varepsilon nFc_F D_o}{s_R \kappa}} \frac{Sh}{Pe^2} = \frac{1}{2}(\alpha d)^2 \,. \quad (22)$$

The solution obtained by Fedkiw which includes the effects of the finite electrode length can be represented as

$$\frac{\Phi_2(x=0,y=0) - V}{\dfrac{nFc_F v^2}{s_R \kappa a k_m}} = \frac{\Delta\Phi_2}{\dfrac{\varepsilon n F c_F D_o}{s_R \kappa}} \frac{Sh}{Pe^2} = f(\alpha d, \alpha L) \tag{23}$$

where $f(\alpha d, \alpha L)$ represents a complicated function of the variables αd and αL previously derived by Fedkiw [8].

For the flow–through electrode, the maximum solution phase potential drop occurs between the front and the rear of the electrode, $y=0$ and $y=L$. From Bennion and Newman [1], this is

$$\frac{\Phi_2(y=0) - \Phi_2(y=L)}{\dfrac{nFc_F v^2}{s_R \kappa a k_m}} = \frac{\Delta\Phi_2}{\dfrac{\varepsilon n F c_F D_o}{s_R \kappa}} \frac{Sh}{Pe^2} = 1 - e^{-\alpha L}\left(1 + \alpha L\right). \tag{24}$$

In Figure 2 we have plotted the dimensionless maximum potential drop times the ratio of the Sherwood Number to the square of the Péclet Number for a flow–by electrode. The variable αd has been chosen as the independent variable. We have included curves for a semi–infinite electrode and curves for electrodes of finite aspect ratio. Curves for the finite aspect ratio electrodes were obtained from the work of Fedkiw. In addition, the solution given by Alkire and Ng is shown. These curves are independent of any specific mass–transfer relationship. This figure clearly demonstrates five points.

(1) The dimensionless maximum potential drop times the ratio of the Sherwood Number to the square of the Péclet Number calculated by the finite–electrode solution, the semi–infinite–electrode solution, and the Alkire and Ng solution all approach the same limit as αd becomes small.

(2) The maximum dimensionless potential drop times the ratio of the Sherwood Number to the square of the Péclet Number approaches a

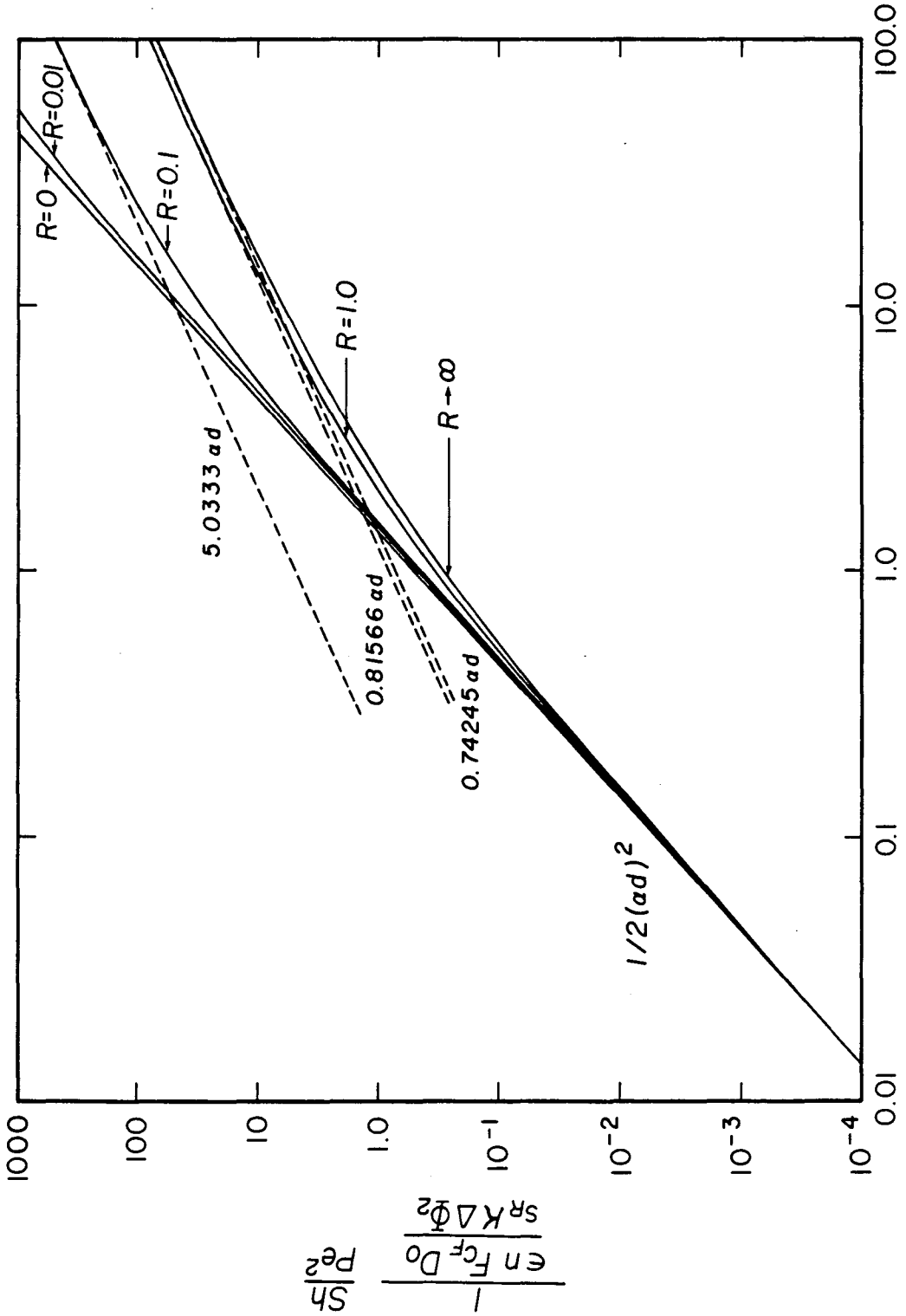

XBL 841-324

Figure 2

limit for R becoming large. At large values of αd and large aspect ratios this relationship becomes proportional to αd. In the limit of small αd, this relationship approaches a value given by $1/2(\alpha d)^2$.

(3) The maximum dimensionless solution phase potential drop times the ratio of the Sherwood Number to the square of the Péclet Number for finite R asymptotically becomes proportional to αd at large values of αd. The value of this proportionality constant is determined by the magnitude of R.

(4) The effect of the finite electrode length is important only for values of R approximately less than one and then only at large values of αd.

(5) The Alkire and Ng one–dimensional solution is seen to reflect the limit as the aspect ratio of the flow–by electrode tends toward zero for all values of αd. This contrasts with earlier work which has assumed the Alkire and Ng solution results only as the aspect ratio R, goes to infinity [8].

If the maximum dimensionless solution phase potential drop times the ratio of the Sherwood Number to the square of the Péclet Number for the flow–through electrode were plotted on this graph, the resulting curves would be horizontal straight lines. Equation (24) shows that for the flow–through electrode this quantity is not dependent upon the parameter αd.

Comparison of Configurations

As a first approximation, the optimum electrode configuration for a specified conversion might be found by assuming that the dimensionless potential drops times the ratio of the Sherwood Number to the square of the Péclet Number are equal. This would correspond to both the flow–through and flow–by electrodes having identical volumes, flow–rates, and consequently, equal pressure drops. In Figure 3 we have plotted the values of αd and R (as functions of αL) which give equal dimensionless maximum potential drops times the ratio of the Sherwood Number to the square of the Péclet Number for the flow–through electrode and for the flow–by electrode. We have also designated the regions where each type of configuration is preferred. Again, the variable αL directly represents the requirement of conversion that we have imposed on the design. The maximum dimensionless potential drop times the ratio of the Sherwood Number to the square of the Péclet Number for the flow–through electrode has been calculated using Equation (24). We have included the three possibilities for evaluating the this quantity for the flow–by electrode. First, the flow–by electrode is assumed to be infinitely long, and Equation (21) is used. We can also assume the one–dimensional potential variation of Alkire and Ng might be appropriate and use Equation (22). Finally, the effects of the finite electrode length also can be included. The relationship given by Fedkiw could also be used. For this finite electrode case, an additional constraint must be imposed since this function explicitly depends on the aspect ratio. The value of R is computed from

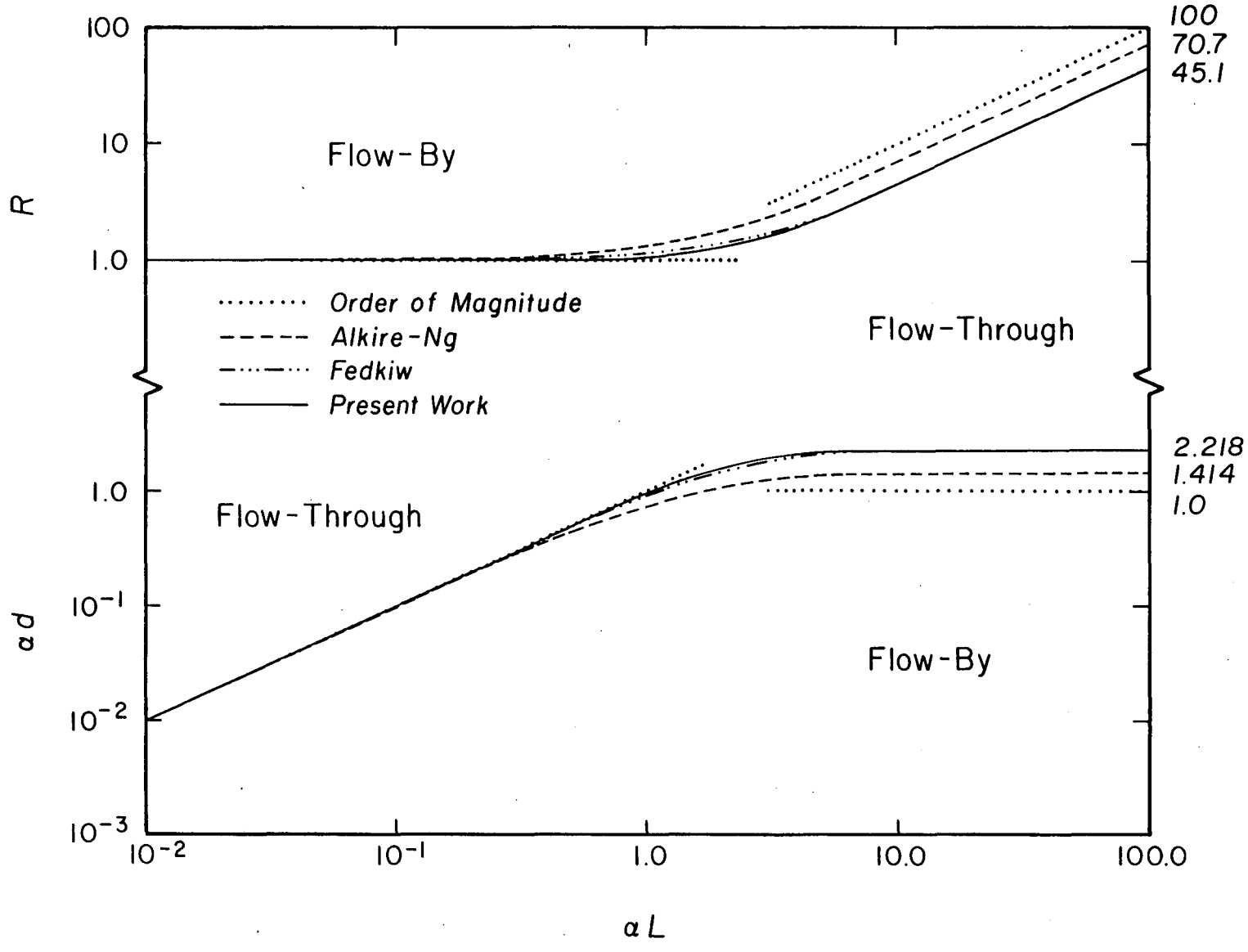
100
10
1.0
R
Flow-By
Order of Magnitude
Alkire-Ng
Fedkiw
Present Work
Flow-Through
100
70.7
45.1
2.218
1.414
1.0
1.0
10^{-1}
10^{-2}
10^{-3}
αd
Flow-Through
Flow-By
10^{-2}
10^{-1}
1.0
10.0
100.0
αL
XBL 841-325

Figure 3

$$R = \frac{L}{d} = \frac{\alpha L}{\alpha d} . \tag{25}$$

Thus, the value of αd and the value of R is found for each value of αL such that the maximum dimensionless potential drops times the ratio of the Sherwood Number to the square of the Péclet Number are equal. For comparison, we have also included the results of the order of magnitude analysis which were derived in the introduction.

We emphasize here, that this comparison of the two electrode configurations does not require that we specify a mass–transfer coefficient relationship. This comparison does not depend upon the Sherwood–Péclet Number relationship. Fedkiw compared the two configurations in a similar way except that he introduced a specific Sherwood–Péclet Number relationship in his comparison. The comparison presented here is considered to be preferable because it is not restricted to a single correlation.

Figure 3 establishes several important points. At low values of αL and, consequently, low conversion, the aspect ratio and the value of αd for equal potential drops are independent of the flow–by potential drop relationship. The Alkire and Ng one–dimensional approximation, the semi–infinite electrode approximation, and the finite electrode relationship all predict the same geometry. In this low conversion range, αL less than one, the aspect ratio for equal potential drops is seen to approach one. The value of αd, given equal electrode cost, is seen to approach a limiting relationship of

$$\alpha d = \alpha L . \tag{26}$$

The conclusion to be made here is that a flow–by electrode is favored at low conversions if it can be constructed with an aspect ratio greater than one. Otherwise, a flow–through electrode would be a better choice. Equation (26)

is identical to Equation (2) obtained by the order of magnitude analysis in the introduction section.

At higher conversions, values of αL greater than about 2, the criterion that specifies the more economical configuration changes. In this region, the value of R delineating the optimum electrode configuration no longer is constant. Also, the one–dimensional Alkire and Ng approximation deviates from the two–dimensional solutions. Since the one–dimensional approximation over-predicts the potential drop, it results in a criterion giving a lower flow–by aspect ratio. The two–dimensional potential distributions are thus seen to affect the choice of electrode configurations only at high conversions. From Figure 3 we can see that at high conversion one would choose a flow–by electrode only if the resulting aspect ratio is greater than 0.45 times αL. According to Fedkiw [8], the flow–by configuration was preferred over the flow–through configuration for

$$R \geq 5 \,. \tag{27}$$

One can see, however, that this relationship holds only for values of αL near 10. In terms of αd, the flow–by electrode is superior at high conversions only if

$$\alpha d < 2.218 \,. \tag{28}$$

Except for the factor of 2.218, Equation (28) is consistent with Equation (1) obtained by an order of magnitude estimate in the introduction section. This factor accounts for the variation of current across the flow–by electrode and the two–dimensional current flow which was not included in the earlier analysis.

Figure 3 also demonstrates another significant point. The curves for the optimum electrode configuration given by the finite length electrode or

the semi–infinite electrode are very nearly the same. At high and low conversions, the criterion becomes independent of whether one considers the finite electrode length. Only for a region of αL near one, does the effect of the finite electrode length on the criterion become noticeable. From Figure 2, one can see that only when the aspect ratio approaches one at high conversions does the effect of the finite electrode length on the potential drop become noticeable. But at large conversions, or large αL, it is impractical to construct a flow–by electrode with an aspect ratio near one. Consequently, considering the potential distribution in a flow–by electrode of finite length is not really important for practical flow–by designs when the maximum potential drop is used as a basis for comparison. The potential distribution for an electrode with an infinite aspect ratio gives results which are practically identical but in a less complicated expression.

Conclusions

The two–dimensional potential distribution for a flow–by porous electrode of infinite length to width ratio operating at the limiting has been derived. It is shown that the maximum solution phase potential drop depends primarily on the ratio of the electrode width and the penetration depth αd. The potential drop for practical flow–by designs depends only weakly upon the length to width ratio. This result has been compared to the potential drop for a finite length electrode given by Fedkiw and the one–dimensional potential drop of Alkire and Ng.

The flow–through and flow–by electrode configurations have been compared at the limiting current using the maximum solution phase potential difference as a basis for comparison. This comparison is independent of any specific mass–transfer coefficient correlation. Criteria delineating the optimal electrode configuration have been given which depend upon the reactant conversion. At low conversion a flow–by electrode is favorable providing that it can be constructed with a length to width ratio greater than one. At high conversions, however, a flow–by electrode is favorable if the ratio of the electrode width and penetration depth is less than 2.218.

Acknowledgement

This work was supported by the Assistant Secretary of Conservation and Renewable Energy, Office of Energy Systems Research, Energy Storage Division of the U.S. Department of Energy under Contract DE-AC03-76SF00098.

List of Symbols

English Characters

a	specific interfacial surface area, cm^2/cm^3
c	pore averaged concentration, $mole/cm^3$
d	flow–by electrode bed width perpendicular to fluid–flow direction, cm
D_o	free stream diffusion coefficient of reacting species, cm^2/s
F	Faraday constant, 96,485 coulombs/equiv
i_2	total current density within electrolyte phase, A/cm^2
j	transfer current density, A/cm^3
k_m	mass transfer coefficient, cm/s
L	bed depth in direction of fluid flow, cm
M	arbitrary species
n	number of electrons transferred in reaction
Pe	Péclet number, v/aD_o
R	bed aspect ratio, L/d
Sh	Sherwood number, $\varepsilon k_m/aD_o$
s_R	stoichiometric coefficient of reactant
v	superficial fluid velocity, cm/s
V	reference potential of flow–by electrode at $y=d$, V
z	charge number, equiv/mol

Greek Characters

α	reciprocal of penetration length, ak_m/v, cm^{-1}
$\Delta\Phi_2$	maximum allowable solution potential drop, V
ε	bed porosity or void fraction

κ	conductivity of fluid phase in bed, $(\Omega cm)^{-1}$
λ	dimensionless eigenvalue
Φ_2	solution potential, V

Subscripts

i	species number
n	eigenvalue number
F	feed condition
L	exit condition

Figure Captions

Figure 1. Porous electrode configurations, a) flow–through electrode, upstream counterelectrode, b) flow–by electrode.

Figure 2. Dimensionless maximum potential drop times the ratio of the Sherwood Number to the square of the Péclet Number for the flow–by electrode of various aspect ratios as a function of αd.

Figure 3. Values of αd and R for equal dimensionless potential drops times the ratio of Sherwood Number to the square of the Péclet Number for the flow–through electrode and the flow–by electrode using: a) order of magnitude expressions, b) Alkire and Ng expression, c) semi–infinite electrode, d) Fedkiw expression. These two representations are equivalent since $R = \alpha L / \alpha d$.

References

(1) Douglas Bennion and John Newman, "Electrochemical removal of copper ions from very dilute solutions," *J. Appl. Electrochem.*, **2**, 113–122 (1972).

(2) J. L. Fitzjohn, "Electro–organic Synthesis," *Chemical Engineering Progress*, **71**, 85–91 (1975).

(3) James A. Trainham and John Newman, "A Comparison Between Flow–Through and Flow–By Porous Electrodes For Redox Energy Storage," *Electrochimica Acta*, **26**, 455–469 (1981).

(4) James A. Trainham and John Newman, "The Effect of Electrode Placement and Finite Matrix Conductivity on the Performance of Flow–Through Porous Electrodes," *J. Electrochem. Soc.*, **125**, 58–68 (1978).

(5) James A. Trainham and John Newman, "A Flow–Through Porous Electrode Model: Applications to Metal–Ion Removal from Dilute Streams," *ibid*, **124**, 1528–1539 (1977).

(6) Richard Alkire and Patrick Ng, "Two–Dimensional Current Distribution Within a Packed–Bed Electrochemical Flow Reactor," *ibid*, **121**, 95–103 (1974).

(7) Richard Alkire and Patrick Ng, "Studies on Flow–By Porous Electrodes Having Perpendicular Directions of Current and Electrolyte Flow," *ibid*, **124**, 1220–1227 (1977).

(8) Peter Fedkiw, "Ohmic Potential Drop in Flow–Through and Flow–By Porous Electrodes," *ibid*, **128**, 831–838 (1981).

(9) John Newman and William Tiedemann, "Flow-through Porous Electrodes," *Advances in Electrochemistry and Electrochemical Engineering*, Vol. 11, Heinz Gerischer and Charles Tobias, eds., Wiley Interscience, New York (1978).

TECHNICAL INFORMATION DEPARTMENT
LAWRENCE BERKELEY LABORATORY
UNIVERSITY OF CALIFORNIA
BERKELEY, CALIFORNIA 94720